2D.1 DETERMINATION OF A CONSISTENT TIME FOR THE EXTRATROPICAL TRANSITION OF TROPICAL CYCLONES

David E. Kofron*, Elizabeth A. Ritchie, and J. Scott Tyo
University of Arizona, Tucson, Arizona

1. INTRODUCTION

Although there has been considerable research on tropical cyclones (TCs) and extratropical cyclones, the transition of TCs as they propagate into the mid-latitudes and interact with extratropical features has received somewhat less attention. Many of these TCs become powerful extratropical cyclones, and they often pose a threat to marine interests and countries in a similar fashion as TCs.

The process by which a TC moves poleward, loses tropical characteristics, and interacts with the mid-latitude environment is called extratropical transition (ET). Some of the environmental changes include an increase in vertical wind shear associated with increasing mid-latitude westerlies and baroclinicity, stronger meridional temperature gradients, a decrease in sea surface temperatures (SST's) with an increase in the SST gradient, and an increase in the Coriolis parameter (Jones et al. 2003). The effects of these environmental changes are generally to increase the translation speed of the storm while decreasing the maximum wind speed but increasing the size of the storm. The increase in the size and speed along with increased environmental westerly vertical shear causes the decaying TC to become very asymmetric and contributes to the generation of large waves and swells (Jones et al. 2003). Because there is no clear understanding of how the TC and mid-latitude features interact, it is difficult to forecast the ensuing intensity of the fully transitioned extratropical cyclone. It is also problematic to accurately forecast the speed and location of the storm because small errors in the initial location of the TC can result in large errors in the 24 and 48-hour numerical weather prediction forecast. These basic forecasting issues make it challenging to forecast the location of the high winds and precipitation and the oceanic response to the transitioned cyclone (Jones et. al. 2003).

In order to better forecast the extratropical transition of TCs, it would be useful to identify a focal time for all cases of ET at which the TC loses tropical characteristics and begins to interact with the preexisting mid-latitude cyclone or trough. This time is called the "ET time" in this study. Although there has been a recent increase in the study of physical processes associated with TCs as they transition into extratropical cyclones, no common definition of ET exists that is consistent across all cases. Such a definition would have utility for the operational community by providing a standardized time to designate extratropical transition. There would also be several benefits for the research community, including a consistent designation in the best track records for ET with associated criteria that are physically based but easily understood.

The existing definitions of ET include, but are not limited to, descriptions of the structural evolution of the TC during extratropical transition using satellite derived data (Klein et al. 2000), analyses (Sinclair 2002; Foley and Hanstrum 1994) and gridded datasets (Ritchie and Elsberry 2001, 2003, and 2007; Demirci et al. 2007), the progression of an axisymmetric warm- core system to an asymmetric cold-core system via phase-space (Hart and Evans 2003; Evans and Hart 2003), and frontogenesis (Harr and Elsberry 2000).

A potentially useful tool for determining the ET-time is potential vorticity (PV). The idea of "PV thinking" has been discussed (Jones et al. 2003), but it has not been used as a means of characterizing the evolution of a TC undergoing ET. Like phase-space, PV can be used to explain the structure of the TC and the balanced atmospheric flow surrounding the TC. The values decrease quickly out from the center, and the PV gradients relax as well. The preexisting trough that the TC interacts with has higher PV values in the upper levels because the upper level jet is dominant. Some more mature mid-latitude cyclones may also exhibit higher low-level PV values along a frontal boundary. The interaction of the TC and the trough may be best explained by examination of mid-level isentropic PV (IPV).

In this study, we will examine the potential usefulness of potential vorticity diagnostics for both describing the physical evolution of TCs

*Corresponding author address: David E. Kofron, Univ. of Arizona, Dept. of Atmospheric Science, Tucson, AZ 85721-0081.
email: kofron@atmo.arizona.edu.

undergoing ET and defining an ET time that useful to both the operational and research communities.

2. DATA AND METHODS

The data used are the Naval Operational Global Atmospheric Prediction System (NOGAPS) analyses on a 1° lat-lon grid at 13 levels between 1000 and 100 hPa. Recurving TCs from the northwest Pacific and north Atlantic oceans from 2003 through 2006 (82 storms) are included in the dataset. For each storm, the 6 days surrounding a first guess ET time, which is defined as the time at which the TC becomes an open wave in the 500-hPa geopotential height analyses at 12-hour intervals, are included. After each storm center is accurately found, the data are storm-centered on an 83° by 73° grid. The data are then used to calculate the absolute potential vorticity (PV) along constant pressure surfaces by

$$PV = \frac{1}{\rho}(\zeta + f)\nabla\theta$$

where ρ is the density of air, ζ is the relative vorticity, f is the Coriolis parameter, and θ is potential temperature. Through the ideal gas law and other mathematical arrangements, the isentropic potential vorticity (IPV) along constant potential temperature surfaces can be calculated by

$$IPV = -g\left(\zeta_\theta + f\right)\frac{\partial\theta}{\partial z}$$

where g is gravity and ζ_θ is relative vorticity along a constant potential temperature surface. For all storms at all times, the circular average of PV and IPV are calculated within a storm-centered circle with a radius of 500 km.

The 2003 through 2006 seasons are chosen because the number of recurving TCs (82) is deemed a sufficient size to separate into different scenarios based on the TC and trough interaction. The three main scenarios include storms that undergo ET and reintensify, storms that undergo ET but dissipate, and storms that recurve but do not interact with any mid-latitude feature and do not undergo ET. In order to determine post-transition reintensification, the change in sea level pressure is examined at the center of the cyclone and for the surrounding environment. Reintensification is then defined as a decrease of 3 hPa or greater of the difference between the environmentally averaged sea level pressure and the minimum central pressure of the cyclone. By this definition, 58 of the 82 TCs examined reintensified post-transition. Further examination

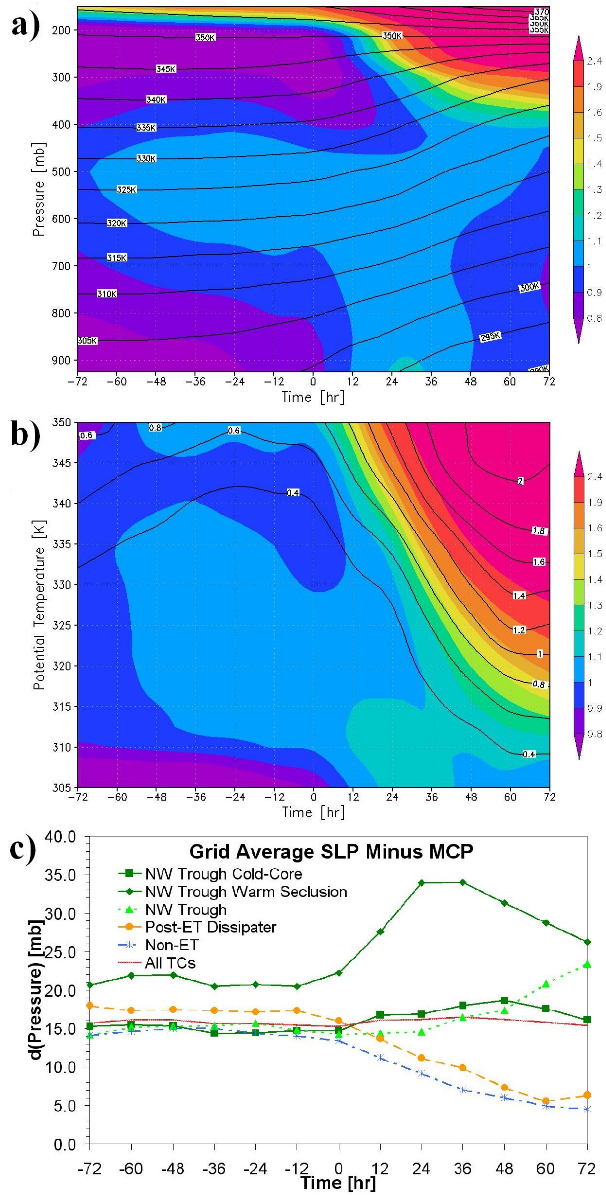

Figure 1: Time series centered on the 500-hPa geopotential height open wave time for: a) the average of circularly averaged PV (PVU, shaded) and potential temperature (K, contour) for all recurving cases; b) average (PVU, shaded) and standard deviation (PVU, contour) of the circularly averaged IPV for all recurving TCs; and c) average difference of the grid-averaged sea-level pressure and the minimum central pressure for each scenario and all TCs.

of the TCs reveals that 16 did not undergo ET, which leaves 8 TCs that weakened (or dissipated) post-transition.

The 58 post-transition reintensification cases are further separated into two scenarios based on their interaction with a preexisting mid-latitude cyclone to the northeast or northwest. This is determined by examination of the 500-hPa analyses, as suggested by Harr and Elsberry (2000). Most of the TCs (42) are accelerated by a preexisting mid-latitude cyclone to the northwest and either undergo ET as cold-core transition storms (33) or as warm-seclusion transition storms (9). The distinction between cold-core and warm seclusion evolution transitions is found by the use of cyclone phase-space (Hart and Evans 2003). The other reintensifying TCs (16) are accelerated rapidly by the westerly flow and interact with the mid- latitude cyclone to the northeast. All of the TCs that interact with a downstream trough undergo cold-core transitions.

3. RESULTS

3.1 PV versus IPV evolution of ET cases

During ET, the atmospheric flow around TCs changes dramatically. The average potential temperature and PV for all 82 cases plotted versus pressure are shown in Fig. 1a. The potential temperature is averaged within a TC-centered 5° latitude by 5° latitude box, the PV is circularly averaged within a 500 km radius of the TC center, and the time series is centered on a first-guess ET time, which is taken as the time when the TC appears as an open wave in the 500-hPa geopotential height field (Demirci et al. 2007).

In order to begin examination of ET by potential vorticity, it is important to determine which isentropic levels appear to have the greatest impact. Figure 1a shows that, on average, the potential temperature decreases with time for recurving TCs and the largest PV values are between the 700 mb and 400 mb pressure levels. Below 700 mb, the potential temperature and PV values remain relatively constant prior to becoming an open wave. After the 0-h time, the average PV values reach a maximum between +12-h and +48-h and the potential temperature decreases due to the general northward propagation of the TC. At the 850 mb level, the potential temperature decreases from 305 K to about 295 K, and a decrease of about 10 K can be seen at all pressure levels up to approximately 250 mb. At about 200 mb, the potential temperature remains mostly constant and above 200 mb, the potential temperature increases with time, so the dynamic tropopause appears to be at or above 200 mb. Between 200 and 400 mb, the PV is constant until the 0-h time and then increases through the end of the period. The increase in PV in the upper troposphere is due to the interaction of the TC with the mid-latitude feature.

On average, the 300 K isentrope does not exist above the 925-hPa pressure level and the tropopause is near 350 K (Fig. 1a), thus IPV is plotted for the isentropic range of 305 K to 350 K(Fig. 1b). The IPV values can be seen in Fig. 1a by tracing the PV along the potential temperature

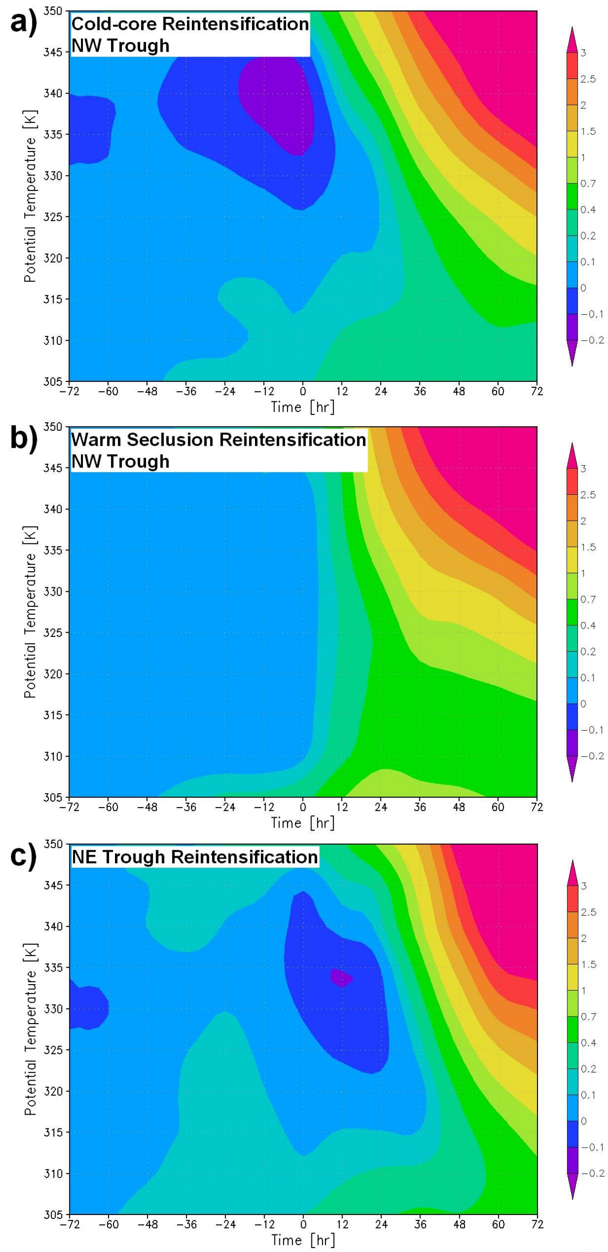

Figure 2: Time series of IPV (PVU) centered on the 500-hPa geopotential height open wave time for: a) cold-core post-ET reintensification cases with a northwest trough; b) warm-seclusion post-ET reintensification cases with a northwest trough; and c) post-ET reintensification cases with a northeast trough.

contours. However, the values in Fig. 1b differ slightly from those in Fig. 1a because of the conservative nature of Ertel's IPV and are more appropriate to examine for an objective measure during ET. For this study, the low-levels are defined as less than 315 K, the upper levels as above 330 K, and the middle level of the atmosphere as the layer in between 315 K and 330 K.

Figure 1b shows the mean and standard deviation of area-averaged IPV plotted on isentropes versus time where the 0-h time refers to the 500-hPa geopotential height open wave time. In the lower levels (below 315 K), the average IPV is relatively low prior to 0-h time, especially below 310 K. At, and subsequent to, the 0-h time the IPV values in the lower levels increase and reach a maximum between +24-h and +36-h. In the middle levels (between 315 K and 330 K), the IPV values are relatively constant before the open wave 0-h time (Fig. 1b) but there is an apparent minimum at the 330-K and 335-K isentropic levels. After the open wave 0-h time, the mid-level IPV begins to increase dramatically as the interaction with the mid-latitude trough strengthens, and the increase occurs earlier at higher isentropic levels. The IPV in the upper levels (above 330 K) is slightly weaker than in the middle levels and remains below 1 PVU before the open wave 0-h time at 340 K and 345 K. At the 350-K isentrope, the IPV values begin to dramatically increase at the open wave time and are the earliest to increase of all the levels examined.

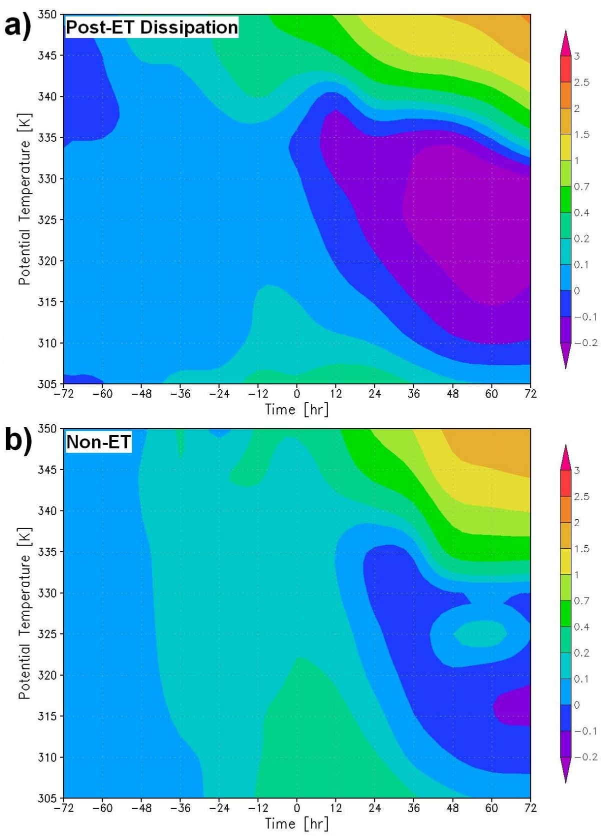

Figure 3: As in Figure 2 for the a) post-ET dissipation cases and b) non-ET cases.

Fig. 1c shows the average time series of grid-averaged sea level pressure minus the minimum central pressure for all 82 TC cases as well as for each of the separated five ET and non-ET scenarios described in KRT. The time series for all cases shows correspondence to the plot of absolute PV with little change in the relative pressure at the surface through the 0-h time, an overall increase to a maximum between +24 and +36 hours when the near-surface PV maximizes, and a gradual decrease subsequently.

Examination of the composite plots of absolute PV and IPV for each of the ET and non-ET cases shows that there is potential discrimination among the different scenarios using these metrics. Figures 2 and 3, for example, show the circularly averaged IPV for the post-transition northwest trough reintensification cases as cold-core systems (Fig. 2a) and warm-seclusion systems (Fig. 2b), the post-transition cases that interact with a northeast trough (Fig. 2c), post-transition dissipation cases (Fig. 3a), and the non-ET recurving TCs (Fig. 3b). The IPV values are plotted as the anomalies to the averages of all cases shown in Fig. 1b. Prior to the 0-h time, the IPV is relatively consistent with the total average for all scenarios. The most obvious difference between the post-ET reintensification cases and the post-ET dissipation cases along with the non-ET cases is the strength and depth of the IPV trough after the 0-h time. In fact, the anomalies for the reintensification cases (Fig. 2) are positive at all levels soon after the 0-h time, and the anomalies for the dissipation cases (Fig. 3a) are negative, especially in the lower and middle levels of the troposphere. The IPV for the non-ET cases (Fig. 3b) after the 0-h time in the lower and middle levels is relatively consistent with the average of all cases because several of the TCs in this scenario reintensify as tropical cyclones as they continue to steer around the ridge. These factors indicate that some IPV metrics may be introduced that can define the beginning and end of ET.

3.2 Defining the "ET time"

The discussion of the IPV evolutions from Figures 2 and 3 suggests it may be possible to use the midlevel IPV to determine the ET time and separate the reintensification cases from the dissipating or non-ET cases. The 330-K isentropic is examined for this purpose. From Figures 2-6, it is found that the 330-K isentropic level begins on average at 500 mb and ends in the time series below the 300-mb level for the reintensification cases, around 450 mb for post-transition dissipation cases, and just above 400 mb for non-ET cases. The differing heights in the atmosphere for each of the categories are simply due to the differing proximities of the TC relative to the trough. Therefore, TCs that remain further south in the northern hemisphere will have isentropic surfaces lower in the atmosphere than TCs that are displaced further north.

At the 330-K isentropic level, the IPV values decrease prior to the open wave time in the 500-hPa geopotential heights. The data for each TC shows that all 82 cases reach a minimum value of 330-K IPV. Figure 4 shows the time series plots of the 315-K and 330-K IPV plotted now using the 330-K IPV minimum time as the 0-h, or ET, time with values all relative to 330-K IPV minimum time value. Therefore, all values are equal to 0 PVU at 0-h. Both images show a large difference between the post-transition reintensification cases and the post-transition dissipation and non-ET cases after

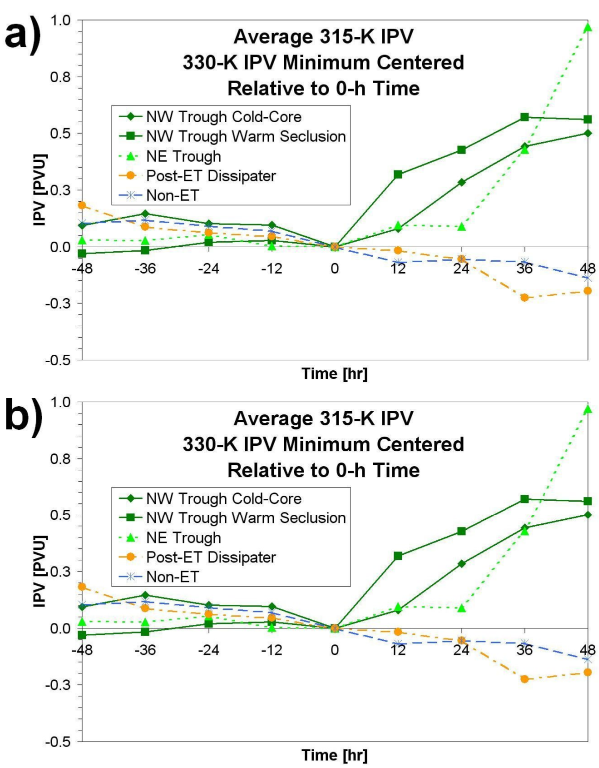

Figure 4: 330-K IPV minimum centered time series relative to their values at the minimum time: a) 315-K IPV; and b) 330-K IPV.

the 0-h time. The reintensification cases rapidly increase at both the 315-K and 330-K IPV levels as the cyclone transitions into an extratropical cyclone. However, the post-ET cases and non-ET cases show a continual decrease of the 315-K IPV values and a general decrease (no great increase) in the 330-K IPV. These results are consistent with the Klein et al. 2000 suggestion that even post-ET dissipation cases should not be considered as ET cases at all. For the following discussion on potential criterion for distinguishing between the scenarios and determining an ET completion time, the post-ET dissipation cases will be treated together with the non-ET cases.

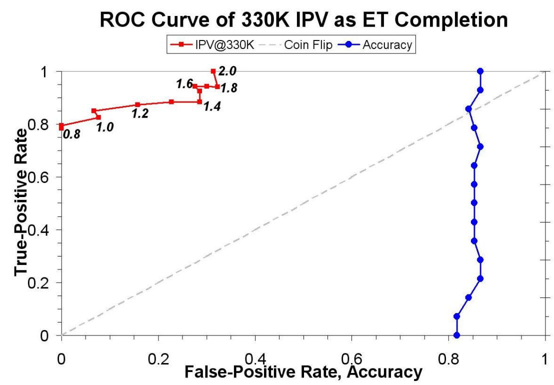

Figure 5: Receiver operater characteristic curve (leftmost y-axis) and corresponding accuracy (rightmost y-axis) of 330-K IPV threshold values.

3.3 Defining an ET completion criteria

An integral part of defining the ET lifecycle is defining the end of the transition period. In order to do so, there must be a more accurate measure for distinguishing between ET and non-ET cases that the 330-K IPV does no accomplish. Furthermore, some criteria must be determined to mark the end of ET. The results shown in Figure 4 lead to the hypothesis that some threshold value of the 330-K IPV may be successful at a) distinguishing ET from non-ET cases and b) defining the end of ET.

The receiver operator characteristic (ROC) is a sensitivity test that can be used for determining the success of different IPV thresholds based on the rate of correctly and incorrectly classified cases. Each case that is successfully captured as ET based on the threshold is called a true-positive, and each case where a TC is falsely classified as ET based on the threshold value is called false-positive. The ultimate goal is to maximize the true-positive rate at the same time as minimizing the false-positive rate. The results of this study are plotted in Figure 5 versus the expectations of a coin flip test, which should yield 50/50 results. The point on the curve closest to the top-left corner has the best accuracy. The accuracy results are plotted based on the rightmost y-axis and reveals that the 1.6 PVU threshold is the most accurate with a rate of 86.6%. IPV thresholds of 0.9 and 1.0 PVU also perform with an 86.6% accuracy, but these values are deemed too low because these values are in the general realm of intensity for all cyclones in the dataset and would not distinguish the storms physically.

4. CONCLUSIONS

This study attempts to alleviate some of the issues with previous methods for determining the lifecycle of a TC undergoing ET by examining PV and IPV as an option for numerically defining the ET onset time and ET completion time, which correspond to the Klein et al. (2000) transformation beginning and end times, respectively. It is found from the time series plots of the circular average of absolute PV that the levels at which the ET is most important are in the middle and upper levels of the atmosphere. These levels translate into isentropic levels as the range between 305 K and 350 K. Further investigation of the time series plots of IPV reveal that the best level for examining ET is at the 330-K potential temperature level because differences in how the low-level atmosphere develops compared with how the upper-level atmosphere develops including the interacting mid-latitude trough are well captured for all scenarios. In general, TCs that enter into the mid-latitude environment and undergo ET show a dramatic increase in the 330-K IPV while TCs that do not interact with mid-latitude features or TCs that dissipate post-transition do not encounter increased IPV values.

A new ET time is determined by using a local minimum value of 330-K IPV as the "IPV-defined" ET onset time. A difficulty arises with this definition of the ET time because: a) there may be more than one minima in any individual recurving TC; and b) there is a reliance on the data at the time before and after the minimum, which means that the ET time can not be determined until after just after it has occurred or must be determined using forecast data. All 82 recurving TCs begin ET using this definition. Examination of the 315-K IPV centered on the 330-K IPV minimum time shows differentiation between the scenarios that complete ET (re-intensifying classes), and those that do not (dissipating and non-ET classes).

An additional way to discriminate these classes of recurving TCs is to numerically define an "ET completion" time. The ET completion time appears to be well defined by the 330-K IPV threshold value of 1.6 PVU with an accuracy of 86.6%. Because there is no need to rely on forecast data or later analyses, the completion of ET can be determined at the moment it occurs. However, it is noted that if the goal was to *predict* the completion of ET, then there would be a need to use forecast fields to determine the threshold. The success rate at which this threshold performs is higher than for the previous methods, and it successfully discriminates between the post-transition reintensification cases and the post-transition dissipation cases and non-ET cases. The likely cause of reaching the threshold or not has to do with the strength of the interaction between the remaining TC and the mid-latitude trough. The dissipation cases and non-ET cases do not interact as strongly with the trough, and therefore, do not reach the threshold value. The average increase in IPV values for these two scenarios is a result of a weak interaction or intensification as a tropical feature after reaching the IPV minimum.

Future work on whether IPV is a useful metric for determining a consistent ET time and providing discrimination among different types of ET will include increasing the number of TCs in the dataset so that a more robust training set can be used. In addition, the work will be extended using analyses that do not include a TC bogus. For this study, it is assumed that the TC bogus in the NOGAPS data has little effect on the data other than better initializing the TC center. Whether this is true may be determined by the use of non-bogus analyses. The goal of all research is to eventually design a forecast model based on statistics that can successfully forecast the ET lifecycle.

Acknowledgements: This work was supported by the National Science foundation under grant ATM-0730079.

5. REFERENCES

Demirci, O., J. S. Tyo, and E. A. Ritchie, 2007: Spatial and Spatiotemporal Projection Pursuit Techniques to Predict the Extratropical Transition of Tropical Cyclones. IEEE Trans. Geo. Remote Sensing, 45, 418-425.

Foley, G. R. and B. N. Hanstrum, 1994: The Capture of Tropical Cyclones by Cold Fronts off the West Coast of Australia. Wea. Forecasting, 9, 577-592.

Evans, J. L. and R. E. Hart, 2003: Objective Indicators of the Life Cycle Evolution of Extratropical Transition for Atlantic Tropical Cyclones. Mon. Wea. Rev., 131, 909-925.

Harr, P. A. and R. L. Elsberry, 2000: Extratropical Transition of Tropical Cyclones over the Western North Pacific. Part I: Evolution of Structural Characteristics during the Transition Process. Mon. Wea. Rev., 128, 2613-2633.

Hart, R. E. and J. L. Evans, 2003: A Cyclone Phase Space Derived from Thermal Wind and Thermal Asymmetry. Mon. Wea. Rev., 131, 585-616.

Jones, S. C., P. A. Harr, J. Abraham, L. F. Bosart, P. J. Bowyer, J. L. Evans, D. E. Hanley, B. N. Hanstrum, R. E. Hart, F. Lalaurette, M. R. Sinclair, R. K. Smith, and C. Thorncroft, 2003: The Extratropical Transition of Tropical Cyclones: Forecast Challenges, Current Understanding, and Future Directions. Wea. Forecasting, 18, 1052-1092.

Klein, P. M., P. A. Harr, and R. L. Elsberry, 2000: Extratropical Transition of Western North Pacific Tropical Cyclones: An Overview and Conceptual Model of the Transformation Stage. Wea. Forecasting, 15, 373-395.

Ritchie, E. A. and R. L. Ellsberry, 2001: Simulations of the Transformation Stage of the Extratropical Transition of Tropical Cyclones. Mon. Wea. Rev., 129, 1462-1480.

---, and ---, 2003: Simulations of the Extratropical Transition of Tropical Cylones: Contributions by the Midlatitude Upper-Level Trough to Reintensification. Mon. Wea. Rev., 131, 2112-2128.

---, and ---, 2007: Simulations of the Extratropical Transition of Tropical Cyclones: Phasing between the Upper-level Trough and Tropical Cyclones. Mon. Wea. Rev., 135, 826-876.

Sinclair, M. R., 2002: Extratropical Transition of Southwest Pacific Tropical Cyclones Part I: Climatology and Mean Structure Changes. Mon. Wea. Rev., 130, 590-609.